02

Influence of the intensity of exciting radiation on the luminescent properties of nanopowders $NaYF_4$: Yb/Tm

© S.A. Burikov[1], E.A. Filippova[1], A.A. Fedyanina[1], S.V. Kuznetsov[2], V.Yu. Proydakova[2], V.V. Voronov[2], T.A. Dolenko[1]

[1] Department of Physics, Moscow State University, Lomonosov Moscow State University, Department of Physics, 119991 Moscow, Russia
[2] Prokhorov General Physics Institute of the Russian Academy of Sciences 119991 Moscow, Russia

e-mail: sergey.burikov@gmail.com

Received December 20, 2021
Revised February 01, 2022
Accepted March 23, 2022

Intensity of the bands of upconversion luminescence of β-$NaYF_4$:Yb^{3+}/Tm^{3+} nanopowders in DMSO suspensions vs intensity of exciting radiation were analyzed. Ranges of changes in the intensity of excitation have been established, in which either the processes of energy transfer from the sensitizer ion to the activator ion or the decay of intermediate levels of activator ions dominate.

Keywords: rare earth ions, upconversion luminescence, nanoparticle suspensions, sensitizer, activator.

DOI: 10.21883/EOS.2022.06.54700.38-22

Introduction

In recent times nanodispersed luminophores based on lanthanide ions have become popular due to the possibility to implement for them the mode of upconversion luminescence under infrared excitation [1]. This provides great opportunities of their use as coding elements [2], photovoltaic devices [3], security printing technology [4], thermometry [5–7], improvement of solar panel performance [8] and in biomedical applications [9–13].

There are several approaches to obtain upconversion luminescence. In the most simple case only one optical center is engaged, that successively absorbs two (several) photons. This method requires high intensities of irradiation (because of small cross-section of two-photon processes), for example, the use of expensive picosecond and femtosecond pulse lasers [14]. An alternative approach is to use nonradiative energy transfer from one center to another luminescence center. Implementation of this approach is based on substances composed of inert matrix doped with two different rare-earth ions (REI). One of them (the sensitizer), with a large absorption cross-section, absorbs the excitation infrared radiation and then transfers the excitation to another ion (the activator) that possesses intense luminescence in visible range. The role of sensitizers is often played by ions of ytterbium, while ions of thulium, erbium or holmium are used as activators [3,5,6,11,15,16]. The role of inert matrices is often played by substances with crystalline structure of gagarinite type: $NaYF_4$ [15,16] or $NaGdF_4$ [17].

Luminescent properties of upconversion luminophores depend on many parameters: intensity of excitation radiation [18,19], temperature [5–7], ratio between concentrations of activator and sensitizer ions [3,11,15,20,21] and the medium where radiating nanoparticles are located [22]. One of the most important among these factors is the intensity of excitation radiation, because the formation of upconversion luminescence is a result of several complex processes taking place during the energy transfer from one type of ions to another. This results in a complex nonlinear behavior of the dependence of luminescence intensity on the intensity of pumping [18,19].

It is found that the efficiency of anti-Stokes luminescence is defined by rates of two competitive processes: nonradiative energy transfer from the sensitizer ion to an intermediate metastable level of the activator ion and the rate of linear decay of this intermediate level [18,19]. In this case, generally the curve of luminescence intensity as a function of pumping power P in the region of low pumping intensity values is described by the P^n function, where n is the number of absorbed photons of pumping required for the upconversion luminescence from the given energy level. With increase in pumping intensity this dependence becomes weaker, down to P^1 [19]. With higher intensities of pumping (tens of W/cm^2) in real systems it is even possible to achieve the effect of luminescence saturation, when slope of the curve of luminescence intensity as a function of pumping intensity in double logarithmic coordinates becomes less than 1 [23].

It should be noted that upconversion luminescence spectra of such ions as erbium, thulium and holmium are composed of a set of bands, each requiring different quantity of pumping photons to obtain a signal. A change in pumping intensity results in change in relative intensity of the spectral bands. This opens up opportunities for a smooth controlled resetting of luminescence color, which

is of major importance for the creation of new radiation sources [24–26].

The nonlinear behavior of dependence of upconversion particle luminescence intensity on the pumping power makes it possible to reduce the size of luminescent spot in the investigations using the method of luminescent microscopy and, in fact, to overcome the diffraction limit [27]. In this case, the bigger is the number of pumping photons required for excitation of the given luminescence band, the better is lateral resolution [27].

The nonlinear behavior of the dependence of upconversion particle luminescence intensity on the pumping power is manifested through the fact that the quantum yield of upconversion luminescence is also nonlinearly dependent on the pumping intensity [28]. This makes it difficult to discuss the quantum yield without connection to the pumping intensity. This situation hampers the characterization of samples and comparison of results obtained in different experiments.

It can be said that the investigation of dependencies of upconversion luminescence intensity of different substances makes it possible to estimate the contribution of particular photophysical processes running under optical excitation, as well as expands the possibilities of their practical use. It should be noted that the authors failed to find in literature the investigation results for the dynamics of optical absorption of REI nanopowders and potential saturation of the absorption in the case of continuous excitation mode and relatively low pumping intensities. It is evident that such studies can provide additional information to understand the processes running in nanopowders with REIs.

In this study we investigated luminescence intensity dependencies of suspensions of β-$NaYF_4:Yb^{3+}/Tm^{3+}$ nanoparticles in DMSO on the pumping power density under continuous laser excitation in the range of $3.5-169.2\,W/cm^2$.

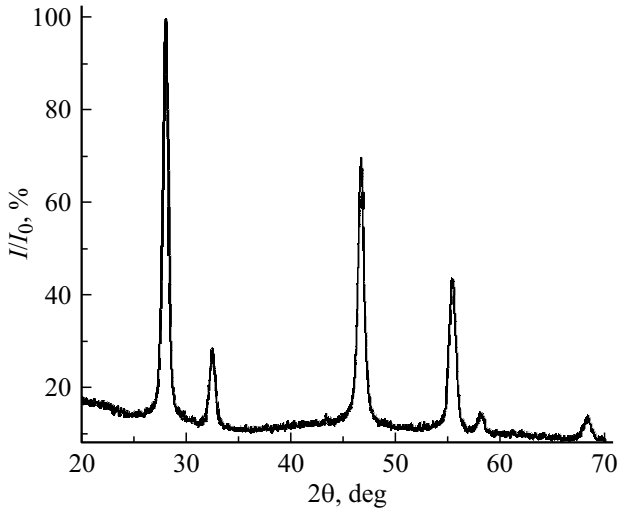

Figure 1. X-ray pattern of β-$NaYF_4:Yb^{3+}/Tm^{3+}$ sample.

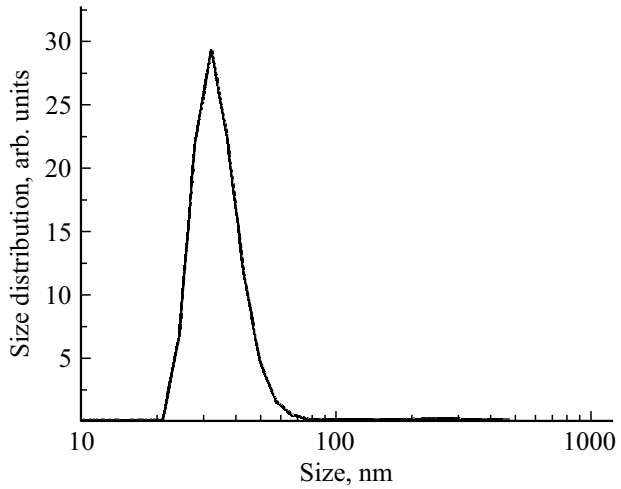

Figure 2. Distribution of particles by sizes according to the DLS data.

Materials and methods

Synthesis and sample characterization

We used suspensions of β-$NaYF_4:Yb^{3+}/Tm^{3+}$ nanoparticles in DMSO as study subjects. The choice of thulium ions as activators is grounded primarily on the fact that thulium has an intense band of luminescence in the transparency window of biological tissue (800 nm). This makes the investigated suspensions promising in terms of biological applications.

β-$NaYF_4:Yb^{3+}/Tm^{3+}$ nanoluminophores were synthesized by solvothermal method in accordance with the procedure described in [6,29]. We used for the synthesis: acetates of yttrium, ytterbium, thulium (99.99%, by Lanhit, Russia), oleic acid (pure grade, by Chimmed, Russia), octadecene (90%, by Sigma Aldrich), NaOH and NH_4F (chemically pure grade, by Lanhit, Russia), methanol (extra pure grade, by Chimmed, Russia), ethanol, chloroform and DMSO (chemically pure grade, by Chimmed, Russia). Concentration of ytterbium was 18.0 mol%, concentration of thulium was 1.0 mol%. Concentration of nanoparticles in the prepared DMSO suspensions was 1 g/l. X-ray pattern of the nanoparticle powder was recorded by a Bruker D8 Advance diffractometer with CuK_α-radiation (Fig. 1). Unit cell parameters ($a = 5.9728(3)$ Å, $c = 3.5153(2)$ Å) were calculated using TOPAS software. They are in line with the data for the undoped sample of $NaYF_4$ from the database of JCPDS 16-0344: $a = 5.96$ Å, $c = 3.53$ Å. No any additional reflexes were detected, which indicates the synthesis of a single-phase sample. The size of coherent scattering area was 15.3(2) nm.

Sizes of nanoparticles in suspensions were measured by the method of dynamic light scattering (DLS) using

Malvern Zetasizer Nano ZS. Average size of aggregates was 36.4 nm (Fig. 2).

The luminescence spectroscopy of suspensions β-$NaYF_4:Yb^{3+}/Tm^{3+}$ in DMSO

To excite a signal of upconversion luminescence, a continuous diode laser was used (with a wavelength of 980 nm). Maximum intensity of radiation was 169.2 W/cm^2. To achieve smooth change in the intensity of excitation radiation, a Thorlabs NDC-500-2 filter with variable absorbance was used. Power of the laser radiation was controlled using an OPHIR thermoelectrical power meter. Samples were probed in a 90-degree geometry of the experiment in a standard quartz cuvette ($10 \times 10 \times 50$ mm). The recording system was composed of an Acton 2500i monochromator (with a focal distance of 500 mm, diffraction grating of 900 lines/mm) and a CCD-camera (Horiba Jobin Yvon, model Syncerity). To suppress the signal of elastic scattering at a wavelength of 980 nm, a blocking interference filter was used.

The luminescence spectrum of β-$NaYF_4:Yb^{3+}/Tm^{3+}$ suspension is composed of a set of bands of different shapes and intensities, that correspond to the following transitions: $^3H_4 \rightarrow {}^3H_6$ (800 nm), $^1G_4 \rightarrow {}^3H_6$ (470 nm), $^1D_2 \rightarrow {}^3F_4$ (450 nm), $^1G_4 \rightarrow {}^3F_4$ (650 nm), $^3F_3 \rightarrow {}^3H_6$ (690 nm) (Fig. 3).

We investigated the luminescence bands with peaks at 800, 470 and 450 nm. This choice was dictated by the considerations of potential practical applications of suspensions. The band in the region of 800 nm (the most intense in the spectrum) is located in the „transparency window“ of biological tissue, which is of interest for biomedical applications, and bands in the region of 470/450 nm correspond to transitions from thermal-bonded levels, which opens the possibility to develop a nanosensor to detect temperature of local environment of nanoparticles. In this study we used a continuous mode of luminescence excitation, and luminescence intensity was determined as the area (sum of samples) under the spectral curve of a luminescence band.

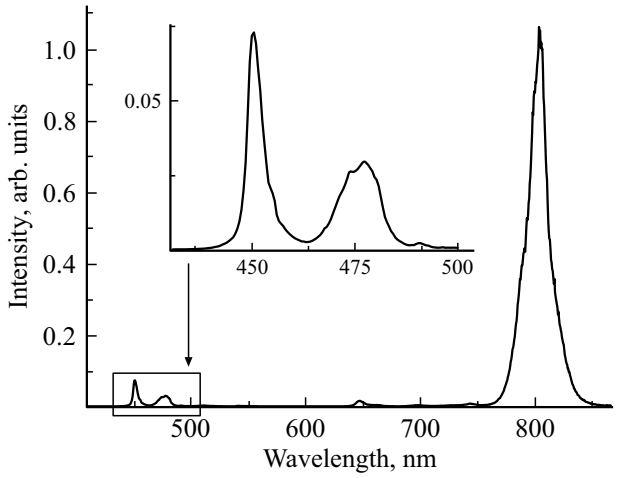

Figure 3. The luminescence spectrum of nanoparticle suspension β-$NaYF_4:Yb^{3+}/Tm^{3+}$ in DMSO

It should be noted that DMSO solvent does not affect the luminescence spectra of nanoparticles, because DMSO has no luminescence in the anti-Stokes region under the excitation by radiation with a wavelength of 980 nm.

Results

Dependence of luminescence intensity of β-$NaYF_4:Yb^{3+}/Tm^{3+}$ suspensions on the intensity of excitation radiation

Luminescence band spectra of suspensions in the region of 450, 470, 800 nm, recorded by CCD-camera at different power levels of the excitation radiation, are shown in Fig. 4.

The obtained dependencies of the integral intensity of selected luminescence bands on the intensity of the excitation radiation are shown in Figs 5–7. The dependencies are represented in linear and logarithmic scales of the excitation radiation intensity.

Behavior of the obtained dependencies can be explained qualitatively taking into account that two types of ions are always present in a nanoluminophore, i.e. activators and sensitizers. The efficiency of anti-Stokes luminescence is defined by rates of two competitive processes: nonradiative energy transfer from the sensitizer ion to an intermediate metastable level of the activator ion and the rate of linear decay of this intermediate level.

This mechanism can be described in a simplified way as follows [28]. The activator is described by a quasi-three-level model: with ground state 0, intermediate state 1 and radiating state 2. States 1 and 2 can represent the set of near energy levels. The activator ion transits from the ground state to state 1 absorbing the energy transferred by nonradiative way from the Yb^{3+} sensitizer ion. Then the activator ion transits to state 2 by means of the second process of energy transfer. The subsequent emission of a photon with anti-Stokes luminescence occurs due to the transition from the second excited state to the ground state.

Behavior of the anti-Stokes luminescence intensity depending on the intensity of laser excitation can be described by the following system of kinetic equations [19]:

$$\frac{dN_{\mathrm{Yb}1}}{dt} = \sigma\rho N_{\mathrm{Yb}0} - \frac{N_{\mathrm{Yb}1}}{\tau_{\mathrm{Yb}1}} = 0, \quad (1)$$

$$\frac{dN_1}{dt} = C_0 N_0 N_{\mathrm{Yb}1} - C_1 N_1 N_{\mathrm{Yb}1} - \frac{N_1}{\tau_1} = 0, \quad (2)$$

$$\frac{dN_2}{dt} = C_1 N_1 N_{\mathrm{Yb}1} - \frac{N_2}{\tau_2} = 0, \quad (3)$$

where $N_{\mathrm{Yb}0}, N_{\mathrm{Yb}1}$ — populations of the ground and excited states of the Yb^{3+} ion, respectively; N_0, N_1, N_2 — populations of the ground, the first, and the second excited states of the activator ion; σ — absorption cross-section of the Yb^{3+} ion; ρ — excitation photon

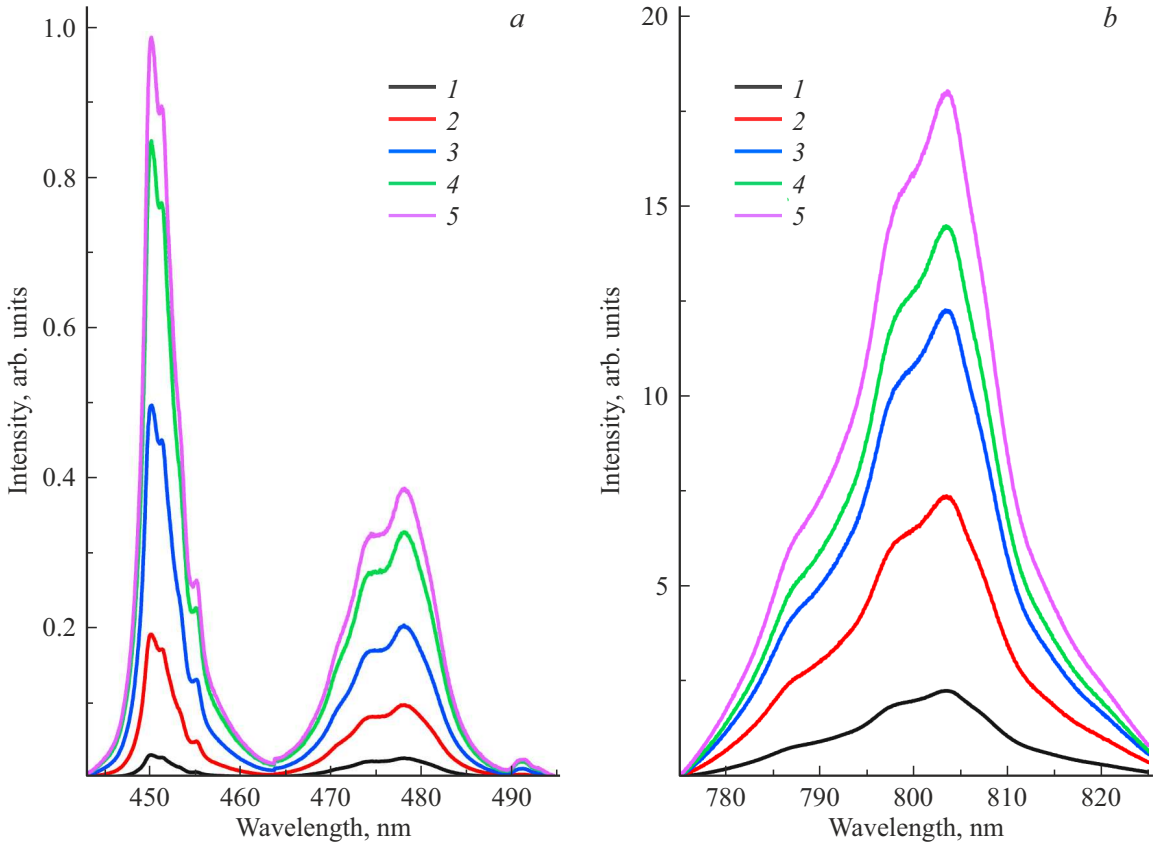

Figure 4. Luminescence spectra of β-$NaYF_4:Yb^{3+}/Tm^{3+}$ suspensions in DMSO at different intensities of excitation radiation: *1* — 39.4 W/cm^2; *2* — 78.9 W/cm^2; *3* — 120.3 W/cm^2; *4* — 145.6 W/cm^2; *5* — 169.2 W/cm^2.

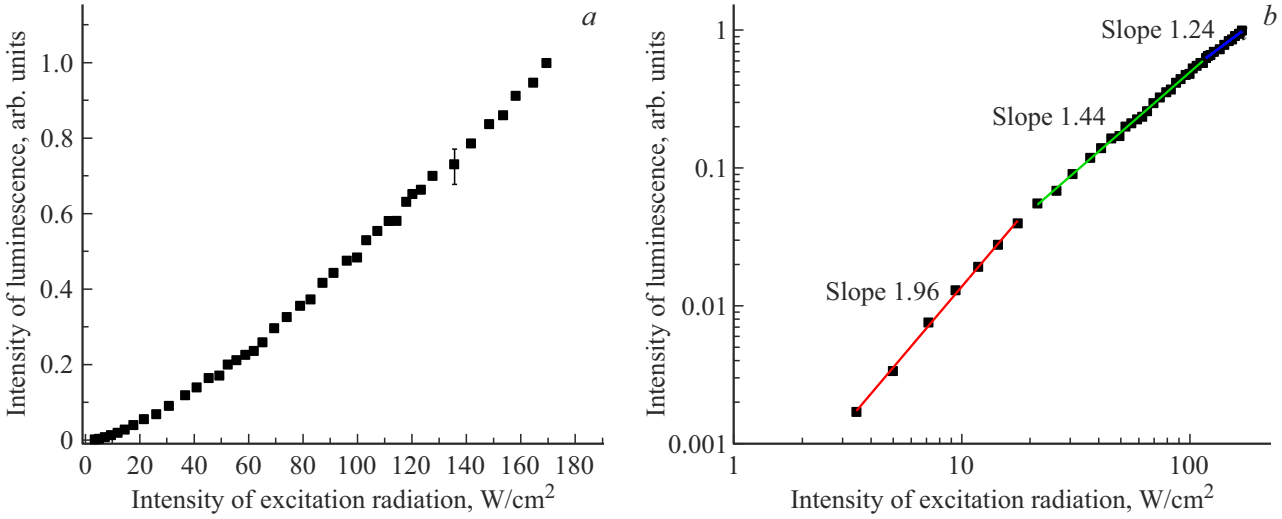

Figure 5. Dependence of integral intensity of the luminescence band at 800 nm on the intensity of excitation radiation (on the left — in linear scale, on the right — in logarithmic scale, with approximations).

flux, which is linearly related to the intensity of excitation radiation; τ_1 and τ_2 — lifetimes of levels 1 and 2 of the activator ion, including the contributions of radiative and nonradiative mechanisms of relaxation; τ_{Yb1} — lifetime of the excited state of the Yb^{3+} ion; C_0, C_1 — constants of the rate of processes of nonradiative energy transfer from the Yb^{3+} ion to the activator ion.

In this model the decay of the excited state of the ytterbium ion ($^2F_{5/2}$ (Yb^{3+})) caused by the energy transfer

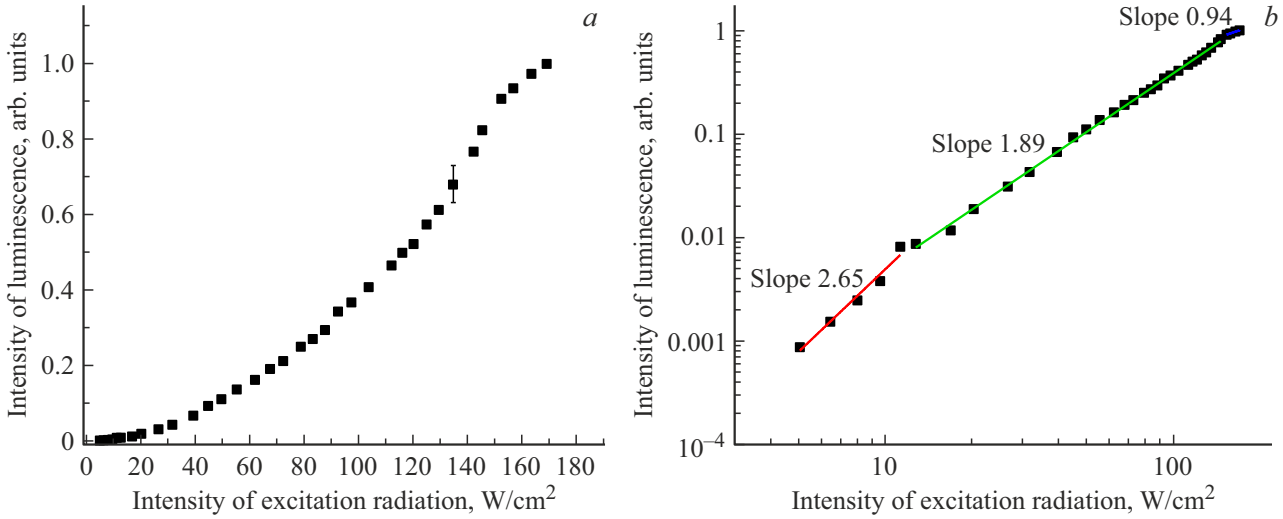

Figure 6. Dependence of integral intensity of the luminescence band at 470 nm on the intensity of excitation radiation (on the left — in linear scale, on the right — in logarithmic scale, with approximations).

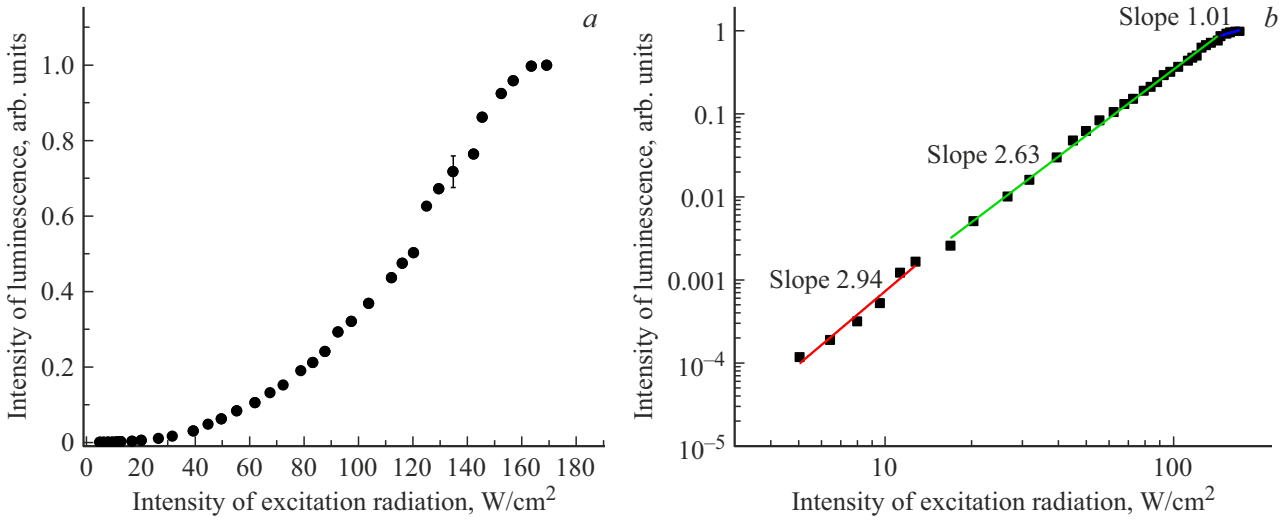

Figure 7. Dependence of integral intensity of the luminescence band at 450 nm on the intensity of excitation radiation (on the left — in linear scale, on the right — in logarithmic scale, with approximations).

to the activator ion can be neglected, because the rate of this process is much less than the rate of the linear decay of this level. Due to the same reason the contribution to the decay of the activator ion level 2 from the process of energy transfer to higher levels is not considered. With these assumptions the expression for the population of the $^2F_{5/2}$ (Yb^{3+}) level is as follows:

$$N_{\mathrm{Yb}\,1} = \tau_{\mathrm{Yb}\,1}\,\sigma N_{\mathrm{Yb}\,0}\,\rho. \qquad (4)$$

Then, the dependence of intensity of anti-Stokes luminescence stationary radiation from state 2 is as follows

$$I = \frac{N_2}{\tau_2^{\mathrm{rad}}}\,h\nu = \frac{C_0 C_1 \tau_{\mathrm{Yb}\,1}^2 \left(\frac{\tau_2}{\tau_2^{\mathrm{rad}}}\right) N_0 h\nu \sigma^2 N_{\mathrm{Yb}\,0}^2 \rho^2}{\frac{1}{\tau_1} + C_1 \tau_{\mathrm{Yb}\,1} \sigma N_{\mathrm{Yb}\,0}\,\rho}, \qquad (5)$$

where τ_2^{rad} — radiative lifetime of state 2, h — the Planck constant, ν — anti-Stokes luminescence radiation frequency.

For improved readability, the data is usually represented in a double-logarithmic scale. In the framework of the developed models of upconversion luminescence formation, the slope coefficient k of the curve of luminescence intensity dependence on the intensity of excitation indicates the multiphoton nature of the excitation of anti-Stokes luminescence radiation. This slope coefficient can be described mathematically as a derivative of $\log I$ with respect to $\log \rho$, i.e.

$$k \equiv \frac{d \log I}{d \log \rho} = 1 + \frac{1}{1 + \tau_1 C_1 \tau_{\mathrm{Yb}\,1} \sigma N_{\mathrm{Yb}\,0}\,\rho}. \qquad (6)$$

Then, according to (6), at a low intensity of the excitation radiation, when the linear decay of the intermediate level of

Slope coefficients of luminescence intensity dependencies on the intensity of excitation radiation

Band of 450 nm		Band of 470 nm		Band of 800 nm	
Intensity of pumping, W/cm^2	Slope coefficient	Intensity of pumping, W/cm^2	Slope coefficient	Intensity of pumping, W/cm^2	Slope coefficient
5.1–12.8	2.94–0.25	5.1–11.3	2.65–0.24	3.5–17.6	1.96–0.04
16.7–145.6	2.63–0.03	13.1–144.9	1.89–0.01	21.6–117.9	1.44–0.01
147.2–169.2	1.01–0.16	152.8–169.2	0.94–0.04	119.7–169.2	1.24–0.04

the activator ion prevails over the process of energy transfer from the sensitizer ion, i.e. when $\frac{1}{\tau_1} \gg C_1 \tau_{\mathrm{Yb}1} \sigma N_{\mathrm{Yb}0} \rho$, the slope coefficient k is equal to 2, which indicates a quadratic dependence of the anti-Stokes luminescence intensity on the excitation intensity, while at high excitation intensities, when the energy transfer from the sensitizer ion plays a considerably more important role, the curve has a slope of 1, i.e. a linear dependence on the excitation intensity takes place. In the intermediate range the slope coefficient varies gradually from 2 to 1 as the excitation intensity increases. It should be noted that in the „balancing point“

$$\rho_b = \frac{1}{\tau_1 C_1 \tau_{\mathrm{Yb}1} \sigma N_{\mathrm{Yb}0}}, \qquad (7)$$

the rate of nonradiative energy transfer and the rate of linear decay contribute equally into the decrease in population of level 1, i.e. $\frac{1}{\tau_1} = C_1 \tau_{\mathrm{Yb}1} \sigma N_{\mathrm{Yb}0} \rho$. Then the curve has a slope of 1.5.

In each of obtained dependencies of the integral intensity of luminescence band on the intensity of excitation radiation we have distinguished three sections differing by slope (Figs 5–7, right). The data was approximated for different sections of intensity curves by the least-square method for linear regression. At each step of the approximation the average error of the approximation was calculated, and an increase in this error signaled the need to proceed to the approximation of the next section of the selected curve. For each region of the intensity curve the slope coefficient was calculated in a logarithmic scale. Results are presented in the table.

For band of 800 nm, at a low pumping power density the slope is approximately equal to 2, i.e. $\frac{1}{\tau_1} \gg C_1 \tau_{\mathrm{Yb}1} \sigma N_{\mathrm{Yb}0} \rho$, and in the given range of intensities the linear decay of the intermediate level of the activator ion prevails over the energy transfer from the sensitizer ion. With high intensities the slope is approximately equal to 1, which indicates that the major role is played by the energy transfer from the sensitizer ion. The intermediate region with a slope of about 1.5 corresponds to the situation when both processes provide approximately equal contributions.

As can be seen, the dependencies for bands in the region of 450 and 470 nm have more complicated behavior (Figs 6, 7). This is related to the fact, that in this case the thulium ion is to be excited to higher energy levels (Fig. 8).

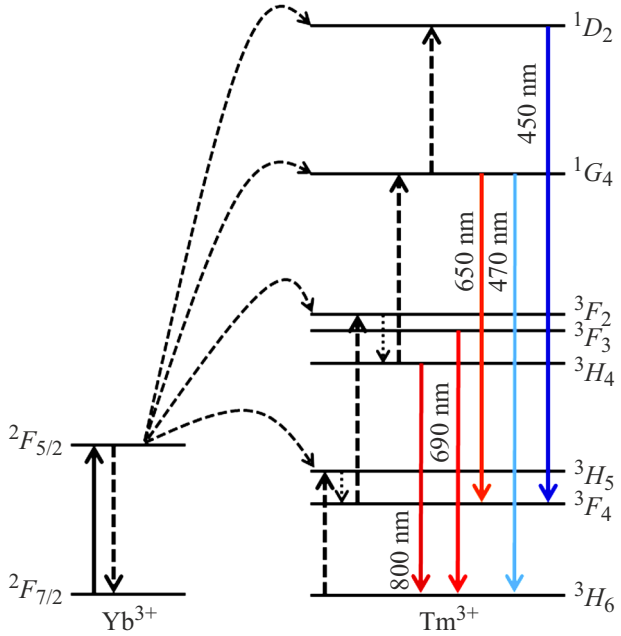

Figure 8. Diagram of energy levels demonstrating the processes running at the upconversion luminescence in $NaYF_4$: Yb, Tm particles.

For this purpose, it is required to engage several excited states of sensitizer ions (pumping photons).

Thus, for the waveband in the region of 470 nm three areas can be distinguished — with slope of 2.65, 1.89 and 0.94 (see the table). Similar to the model suggested for the thulium band at 800 nm, it may be assumed that at low intensities the linear decay of intermediate energy levels prevails, and the luminescence intensity is approximately proportional to the third power of the pumping intensity (because the excitation of luminescence requires three pumping photons (Fig. 8)), at high intensities the curve behavior is defined by the energy transfer from the sensitizer ion and the dependence is linear. The slope coefficient of 1.89 corresponds to the intermediate situation when both these processes have comparable contributions.

For the band in the region of 450 nm the situation is approximately the same with the only difference that in the range of low pumping intensities it could be expected that the luminescence intensity is proportional to the fourth

power of the pumping intensity (in the experiment, a dependence on the third power was observed). This mismatching with the theoretical model can be explained by the fact that it is necessary to take into account the processes of energy transfer from the sensitizer ion, the linear decays of several intermediate levels, as well as the radiating transitions to lower energy states. In addition, it is necessary to take into consideration the potential contribution of cross-relaxation between activator ions. The cross-relaxation is responsible for the concentration extinguishing of the luminescence, because neighboring ions, one of which being in an excited state, while another being in the ground state, exchange the energy in a nonradiative way, usually with following relaxation of phonons [30,31].

Since to form the luminescence band at 450 nm, the maximum number of pumping photons is required, it can be expected that this band is the most sensitive to all processes running with involvement of active rare-earth ions. As a result, the biggest mismatch with the adopted theoretical models can be expected for this band.

Conclusions

Spectra of upconversion luminescence of suspensions based on synthesized nanoparticles of β-$NaYF_4$: Yb/Tm in DMSO were investigated. Dependencies of intensity of three upconversion luminescence bands of thulium (at 450, 470, 800 nm) on the excitation radiation power density ($3.5-169.2\,W/cm^2$) were recorded and analyzed. Ranges of excitation intensity change were identified where prevailing were either the processes of energy transfer from the sensitizer ion to the activator ion or the decay of intermediate levels of activator ion. It is shown that behavior of dependencies for various spectral bands is different from each other. The reason for this is the fact that to excite a luminescence at wavelengths of 450, 470, 800 nm, different numbers of pumping photons are required. The obtained results are important not only for building up theoretical models of photophysical processes in the studied nanopowders, but also for their successful application in practical biomedical tasks, technologies, etc.

Funding

This study was supported financially by the Theoretical Physics and Mathematics Advancement Foundation „BASIS“ (project 21-2-9-21-1 (E.A. Filippova)) with support of the Interdisciplinary Research and Education School of the Moscow University „Photonic and Quantum Technologies. Digital Medicine“.

Conflict of interest

The authors declare that they have no conflict of interest.

References

[1] F. Auzel. J. Lumin., **223**, 116900 (2020). DOI: 10.1016/j.jlumin.2019.116900
[2] Q. Liu. *Studies of optical properties of lanthanide upconversion nanoparticles for emerging applications.* Ph.D. Thesis (Sweden: KTH Royal Institute of Technology, Stockholm, 2020), pp. 73. URL: https://www.diva-portal.org/smash/get/diva2:1429054/SUMMARY01.pdf
[3] S. Han, R. Deng, X. Xie, X. Liu. Angew. Chem. Int. Ed., **53**, 11702 (2014). DOI: 10.1002/anie.201403408
[4] M. You, J. Zhong, Y. Hong, Z. Duan, M. Lin, F. Xu. Nanoscale, **7**, 4423 (2015). DOI: 10.1039/c4nr06944g
[5] O.E. Sarmanova, S.A. Burikov, K.A. Laptinskiy, O.D. Kotova, E.A. Filippova, T.A. Dolenko. Spectrochim. Acta, Part A, **241**, 118627 (2020). DOI: 10.1016/j.saa.2020.118627
[6] D. Pominova, V. Proydakova, I. Romanishkin, A. Ryabova, S. Kuznetsov, O. Uvarov, P. Fedorov, V. Loschenov. Nanomaterials, **10**, 1992 (2020). DOI: 10.3390/nano10101992
[7] D. Jaque, F. Vetrone. Nanoscale, **4**, 4301 (2012). DOI: 10.1039/C2NR30764B.
[8] A. Shalav, B.S. Richards, M.A. Green. Sol. Energy Mater. Sol. Cells, **91**, 829 (2007). DOI: 10.1016/j.solmat.2007.02.007
[9] A. Escudero, A.I. Becerro, C. Carrillo-Carrion, N.O. Núñez, M.V. Zyuzin, M. Laguna, D. Gonzalez-Mancebo, M. Ocaña, W.J. Parak. Nanophotonics, **6**, 881 (2017). DOI: 10.1515/nanoph-2017-0007
[10] S.A. Burikov, O.D. Kotova, O.E. Sarmanova, S.V. Kuznetsov, V.Y. Proydakova, V.V. Voronov, P.P. Fedorov, S.V. Patsaeva, T.A. Dolenko. JETP Lett., **111**, 525 (2020). DOI: 10.1134/S0021364020090064
[11] D.V. Pominova, V.Y. Proydakova, I.D. Romanishkin, A.V. Ryabova, P.V. Grachev, V.I. Makarov, S.V. Kuznetsov, O.V. Uvarov, V.V. Voronov, A.D. Yapryntsev, V.K. Ivanov, V.B. Loschenov. Laser Phys. Lett., **17**, 125701 (2020). DOI: 10.1088/1612-202X/abbede
[12] I.N. Bazhukova, V.A. Pustovarov, A.V. Myshkina, M.V. Ulitko. Opt. Spectrosc., **128**, 2050 (2020). DOI: 10.1134/S0030400X20120875
[13] A.A. Skaptsov, S.O. Ustalkov, A.H. Mohammed, A.M. Zakharevich, A.A. Kozyrev, E.A. Sagaidachnaya, V.I. Kochubey. Opt. Spectrosc., **128**, 952 (2020). DOI: 10.1134/S0030400X20070218
[14] F. Auzel. Chem. Rev., **104** (1), 139 (2004). DOI: 10.1021/cr020357g
[15] Y. Hu, Y. Sun, Y. Li, S. Sun, J. Huo, X. Zhao. RSC Adv., **4**, 43653 (2014). DOI: 10.1039/C4RA05205F
[16] A. Pilch, D. Wawrzyńczyk, M. Kurnatowska, B. Czaban, M. Samć, W. Strek, A. Bednarkiewicz. J. Lumin., **182**, 114 (2017). DOI: 10.1016/j.jlumin.2016.10.016
[17] I.D. Kormshikov, V.V. Voronov, S.A. Burikov, T.A. Dolenko, S.V. Kuznetsov. Nanosystems: Physics, Chemistry, Mathematics, **12**, 218 (2021). DOI: 10.17586/2220-8054-2021-12-2-218-223
[18] M. Pollnau, D.R. Gamelin, S.R. Luthi, H.U. Gudel. Phys. Rev. B, **61** (5), 3337 (2000). DOI: 10.1103/PHYSREVB.61.3337
[19] J.F. Suyver, A. Aebischer, S. García-Revilla, P. Gerner, H.U. Güdel. Phys. Rev. B, **71**, 125123 (2005). DOI: 10.1103/PhysRevB.71.125123
[20] C.S. Ma, X.X. Xu, F. Wang, Z.G. Zhou, D.M. Liu, J.B. Zhao, M. Guan, C.I. Lang, D.Y. Jin. Nano Lett., **17**, 2858 (2017). DOI: 10.1021/acs.nanolett.6b05331.

[21] M. Misiak, K. Prorok, B. Cichy, A. Bednarkiewicz, W. Stręk. Optical Materials, **35**, 1124 (2013). DOI: 10.1016/j.optmat.2013.01.002
[22] T. Cong, Y. Ding, S. Xin, X. Hong, H. Zhang, Y. Liu. Langmuir, **32** (49), 13200 (2016). DOI: 10.1021/acs.langmuir.6b03593.s001
[23] J. Zhou, G. Chen, Y. Zhu, L. Huo, W. Mao, D. Zou, X. Sun, E. Wu, H. Zeng, J. Zhang, L. Zhang, J. Qiu, S. XuInten. J. Mater. Chem. C, **3**, 364 (2015). DOI: 10.1039/C4TC02363C
[24] D.L. Gao, X.Y. Zhang, B. Chong, G.Q. Xiao, D.P. Tian. Phys. Chem. Chem. Phys., **19**, 4288 (2017). DOI: 10.1039/c6cp06402g
[25] A. Zhou, F. Song, Y. Han, F. Song, D. Ju, K. Adnan, L. Liu, M. Feng. J. Lumin., **194**, 225 (2018). DOI: 10.1016/j.jlumin.2017.09.055
[26] Z.P. Meng, S.F. Zhang, S.L. Wu. J. Lumin., **227**, 117566 (2020). DOI: 10.1016/j.jlumin.2020.117566
[27] L. Caillat, B. Hajj, V. Shynkar, L. Michely, D. Chauvat, J. Zyss, F. Pelle. App. Phys. Lett., **102**, 143114 (2013). DOI: 10.1063/1.4800445
[28] H.C. Liu, C.T. Xu, D. Lindgren, H.Y. Xie, D. Thomas, C. Gundlach S. Andersson-Engels. Nanoscale, **5**, 4770 (2013). DOI: 10.1039/C3NR00469D
[29] J. Liu, G. Chen, S. Hao, C. Yang. Nanoscale, **9**, 91 (2017). DOI: 10.1039/C6NR08675F
[30] C.S. Ma, X.X. Xu, F. Wang, Z.G. Zhou, D.M. Liu, J.B. Zhao, M. Guan, C.I. Lang, D.Y. Jin. Nano Lett., **17**, 2858 (2017). DOI: 10.1021/acs.nanolett.6b05331
[31] J. Bergstrand, Q.Y. Liu, B.R. Huang, X.Y. Peng, C. Wurth, U. Resch-Genger, Q.Q. Zhan, J.Widengren, H. Agren, H.C. Liu. Nanoscale, **11**, 4959 (2019). DOI: 10.1039/C8NR10332A